European Review for Medical and Pharmacological Sciences 2020; 24: 3215-3222

Protective effect of miR-146 against kidney injury in diabetic nephropathy rats through mediating the NF-κB signaling pathway

H.-Y. YU[1], L.-F. MENG[1], X.-H. LU[1], L.-H. LIU[1], X. CI[1], Z. ZHUO[2]

[1]Department of Nephrology, The Second Hospital of Jilin University, Chang[illegible], China
[2]Department of Cardiology, The Second Hospital of Jilin University, Chan[illegible]un, Ch[illegible]

Abstract. – OBJECTIVE: To study the protective effect of micro ribonucleic acid (miR)-146 against kidney injury in diabetic nephropathy (DN) rats through the nuclear factor-κB (NF-κB) signaling pathway.

MATERIALS AND METHODS: In this experiment, 30 adult Sprague-Dawley rats with 5-6 weeks old and weighing 20-30 g were selected and randomly divided into control group (n=10), model group (n=10), and miR-146 Mimic group (n=10, DN rat model + miR-146 Mimic). The serum levels of creatinine (Cr) and blood urea nitrogen (BUN) in the three groups were [illegible]ed using the full-automatic biochemical [illegible]yzer. The protein expression levels of phos[illegible]r-ylated-inhibitor of NF-κB (p-IκB), p-P65, and Tubulin were detected *via* Western blotti[illegible] The messenger RNA (mRNA) [illegible]65 was d[illegible]termined using quantitative [illegible]e Chain Reaction (qPCR). Positive [illegible]essi[illegible]f p-IκB in tissues was determine[illegible]ing im[illegible]ohisto-chemistry. Moreover, th[illegible]tents [illegible]tory factors tumor ne[illegible]osi[illegible]TNF-α), interleukin-1β (IL-1β), [illegible]IL-6 [illegible]detected using the enzyme-[illegible]d immun[illegible]ent assay (ELISA) kits. Fi[illegible]e apoptosis [illegible]detected through A[illegible]xi[illegible]luorescein isothiocyanate (FITC) al[illegible]propid[illegible]odide (PI) dual-fluorescence [illegible]ling.

RESU[illegible]: The serum lev[illegible]f Cr and BUN were [illegible]ificant[illegible] higher in [illegible]e model group than [illegible]se in [illegible]control group ($p<0.01$), while the[illegible] si[illegible]ficantly [illegible]wer in miR-146 Mimic group [illegible]se in [illegible]model group ($p<0.05$). [illegible] leve[illegible]p-IκB[illegible]d p-P65/P65 significant-[illegible]reas[illegible] model group compared wit[illegible]ose in [illegible]ontrol group ($p<0.01$), while the[illegible]markably declined in the miR-146 Mimic g[illegible]d with those in the model group [illegible].05). [illegible] results of qPCR showed that the [illegible]RNA level of P65 had no significant difference [illegible]g the three groups ($p>0.05$). The immuno-h[illegible]emical assay showed that the positive exp[illegible]ssion of p-IκB in tissues was consistent with those of the protein level as Western blotting revealed. The rats in the model group had evidently in[illegible]d levels o[illegible]IL-1β, and IL-6 comp[illegible]the control[illegible]up ($p<0.01$), while mi[illegible]6 Mi[illegible]roup had evidently decreased levels of the[illegible]mpared with the model grou[illegible]01). Finally, [illegible]tosis was enhanced in [illegible]del group com[illegible]ed with that in the c[illegible]rol group, while it was remarkably inhibited [illegible]e miR-146 M[illegible]c group.

C[illegible]ONCLUSION[illegible]: MiR-146 can inhibit the NF-κ[illegible]naling pat[illegible]y, lower the levels of TNF-α, IL-[illegible]d IL-6[illegible] reduce the apoptosis, thereby ex[illegible]tective effect against kidney injury in DN.

[illegible]:
[illegible]c nephropathy, MiR-146, NF-κB signaling pathway.

Introduction

Diabetes mellitus often leads to microvascular injury, especially microvessels in kidneys, thus causing diabetic nephropathy (DN)[1]. With the improvement of people's living standards in China, the incidence of diabetes mellitus also increases[2]. The chronic development of diabetes mellitus is very harmful. Elevation of urinary protein, glomerular damage, and decline in the glomerular filtration rate are typical manifestations of diabetes mellitus and DN[3]. Therefore, it is extremely important to study the pathogenesis of DN and explore prevention approaches. Previous studies[4,5] have shown that kidney injury in diabetic patients is mainly related to glucose metabolic disorders, oxidative stress, and inflammatory response. Nuclear factor-κB (NF-κB), an important nuclear transcription factor in cells, occupies a pivotal position in the inflammatory signaling pathway. When NF-κB enters the nucleus, the transcription of a variety of cellular inflamma-

Corresponding Author: Zhao Zhuo, MD; e-mail: doctorzhaozhuo@126.com

tory factors can be promoted, thereby mediating the intracellular inflammatory response through inflammatory factors[6].

Besides the NF-κB pathway, many micro ribonucleic acids (miRNAs) are also related to the inflammation. MiRNAs, generally with 19-22 nt in length, are a kind of endogenous non-coding single stranded small RNAs, which can regulate the transcriptional expressions of the target genes[7]. They bind to the 3'-untranslated region (3'UTR) of mRNAs to directly degrade them or inhibit their translation, thereby regulating the gene expressions at the transcriptional level. Important roles of miRNAs in various biological processes have been identified, such as cell differentiation, proliferation, and apoptosis[8-11].

MiR-146 is a widely studied miRNA currently, and its vital function in regulating the innate immunity has been discovered[12]. MiR-146 includes miR-146a located in the second exon on chromosome 5 and miR-146b located on chromosome 10[13]. As a multifunctional miRNA, miR-146 can be involved in a variety of physiological and pathological processes, such as inflammation, immunity, occurrence, and lopment of tumor, by regulating the exp of multiple genes[14-16].

Materials and Me

Animal Modeling and uping

Wild-type Sprague-D (SD) 6 weeks old (Shanghai BR te biolog , Ltd., Shanghai, Chi were the specific pathogen-free ani oom under mperature of 25°C, humid % and 12/12 ght/dark cycle, and the d fr ess to food and water. After habi tion for 1 SD rats were randomly d ed into control model group, and m 46 Mi ic group. In the model group, the were f ith high-glucose high-fat diets for ks d intra toneally injected with 60 mg/ ptozot solution for modeling. lood se el >16.7 mmol/L indicated the cessfu lishment of the DN model. In -146 Mi ic group, the DN model was f in the same way of the model up, and then, DN rats were administrated with R-146 Mimic. In the control group, the same t of normal saline as that in the model gro was injected. All animal operations were performed strictly according to the Guidelines for the Care and Use of Laboratory Animals of the National Institute. This study was approved by the Animal Ethics Committee of Jilin University Animal Center.

Immunohistochemistry of Kidn issue

Bilateral kidneys of rats were t out under anesthesia and washed clean wit al saline. The right kidney was immediatel d with 10% neutral formalin soluti outinely red into paraffin sections, d affinized, inc with methanol contain %-60 H_2O_2 at ro temperature for 30 and ed wi pho-sphate-buffered s e 3 tim Mem-brane permeabi ion wa ducte th 0.1% Triton X 10 S for 20 m they were incubated ormal goat um at room temperatu for 20 rabbit anti-mouse NF-κB p65 monoclonal antib 1:200) in a refrigerator at 4 night, and bio ated goat anti-rabbit I secondary antibody at 37°C for 1 h. After ning with PB for 3 times, the sections were bated with h eradish peroxidase (HRP)-la-b streptavid ntibody at 37°C for 30 min. Aft g in the dark at room temperature, he in counterstaining was conducted for 30 min. The sections were dehydrated in ethanol, transparent with xylene and an with neutral balsam. Finally, the sections were observed under an inverted fluorescence microscope.

The dark brown particles in kidney tissues indicated positive expression. The mean optical density (OD) value of immunohistochemistry-positive particles was determined using ImageJ professional image analysis system. The protein level of phosphorylated-inhibitor of NF-κB (p-IκB) was semi-quantitatively analyzed.

Detection of NF-κB Signaling Pathway in Kidney Tissues using Western Blotting

The kidney tissues of rats were cut into pieces, homogenized, and added with lysis buffer, followed by centrifugation at 20000 g and 4°C for 30 min. The total protein concentration was measured using the bicinchoninic acid (BCA) protein assay kit (Pierce, Rockford, IL, USA). After sodium dodecyl sulphate-polyacrylamide gel electrophoresis (SDS-PAGE), the protein was transferred onto polyvinylidene difluoride (PVDF) membranes (IPVH00010, Millipore, Billerica, MA, USA). The membranes were incubated with primary antibodies p-IκB, p-P65, P65, and Tubulin (CST, Danvers, MA, USA) at 4°C overnight. After being washed, the membranes were

incubated with HRP-conjugated secondary antibodies (CST, Danvers, MA, USA) for 1 h. Finally, the enhanced chemiluminescence (ECL) mixture was added to obtain images using the fluorescence development technique.

Detection of mRNA Expression Level of P65 Via Quantitative Polymerase Chain Reaction (qPCR)

The mRNA was extracted from kidney tissues in each group using the TRIzol reagent (Invitrogen, Carlsbad, CA, USA), and reversely transcribed into complementary deoxyribose nucleic acid (cDNA) according to the instructions. 2 μL of 5×PrimeScript RT Master Mix was added into 500 ng of RNA, and the total reaction system was 10 μL. Then, PCR amplification was performed according to the instructions: 2 μL of cDNA was added with 10 μL of SYBR Premix Ex Taq II (Tli RNaseH Plus) (2×), 0.8 μL of forward primers, 0.8 μL of reverse primers, and 0.4 μL of ROX Reference Dye II (50×), and deionized water was added finally till the total volume was 20 μL. The mRNA expression level was calculated using the cycle threshold, with β-actin as an in[illegible] reference. The primer sequences were as [illegible] P65: F: 5'-CACCAAAGACCCACCTCACC[illegible]R: 5'-CCGCATTCAAGTCATAGTCCC-3', β-a[illegible] F: 5'-GCAGAAGGAGATTACTGCCCT-3', 5'-GCTGATCCACATCTGCTG[illegible]3'.

Detection of Inflamma[illegible] Cyto[illegible]es in Kidney Tissues

A total of 1-5 mg of [illegible]idn[illegible] were [illegible], washed with PBS f[illegible] times, [illegible] with 1-500 μL of radioimm[illegible]recipitation [illegible]y (RIPA) lysis buffer (B[illegible] Shanghai, [illegible]a), and smashed usi[illegible]ne [illegible]genizer, followed by centrifugat[illegible] at 3000 r[illegible]d 4°C for 10 min. Then, th[illegible]pernatant was c[illegible]ed to detect the conte[illegible]f tum[illegible]necrosis fact[illegible]r-α (TNF-α), interl[illegible]n-1β (I[illegible]), and IL-6 *via* enzyme-linked imm[illegible]rb[illegible] assay (ELISA), and quantified based [illegible]protei[illegible]centration in the tissue [illegible]natan[illegible].

De[illegible]tion of [illegible]enal Function in [illegible]

[illegible]erum levels of creatinine (Cr) and blood urea [illegible]rogen (BUN) were detected for reflecting renal [illegible]ions. 4 mL of blood was aseptically drawn fro[illegible]he caudal vein and centrifuged at 3000 g under low temperature for 10 min. The supernatant was collected and placed into the centrifuge tube. Finally, the changes in serum indexes were detected using the full-automatic biochemical analyzer according to the instructions.

Detection of Apoptosis Via Flow Cytometry

The cells were suspended, d[illegible] centrifuged at 1500 rpm for 5 min, and c[illegible]d. The adherent cells were diges[illegible]with try[illegible]on taining ethylenediamine[illegible]acetic acid (E[illegible] for an appropriate ti[illegible]and th[illegible]eaction [illegible] terminated with co[illegible]e m[illegible]m. Th[illegible], the cells were rinsed [illegible]ted, a[illegible]entrifuged at 1500 [illegible]for 5 m[illegible]5×10[illegible]s were collected, re[illegible]nded with [illegible]f binding buffer, an[illegible]d in 5 μL o[illegible]nexin V-Light 650 a[illegible]10 μ[illegible]ropidium iodide (PI) at room temperature in[illegible]k place for 5-15 min. Flo[illegible]metry was pe[illegible]ed within 1 h, and t[illegible]nnexin V-Light 650 fluorescence signal [illegible] detected th[illegible]h the FL4 channel, while the [illegible]uorescence [illegible]al was detected through the [illegible] FL3 cha[illegible]l. The Annexin V-Light 650 sing[illegible]e and PI single positive tube were de[illegible] simultaneously to determine the fluorescence compensation value and the posi[illegible]ross quadrant gate.

Statistical Analysis

GraphPad Prism 6.0 (La Jolla, CA, USA) was used for the statistical analysis of data. The data were expressed as ($\bar{x} \pm s$) and analyzed by *t*-test. $p<0.05$ suggested the statistically significant difference.

Results

Expression of MiR-146 in Each Group

To observe the transfection efficiency of miR-146 Mimic, the expression level of miR-146 was detected. As shown in Figure 1, the expression of miR-146 was significantly upregulated in miR-146 Mimic group, while it significantly declined in the other two groups ($p<0.05$), indicating that subsequent experiments can be performed.

Biochemical Indexes in Kidney Injury in Each Group

The renal function indexes in the three groups were detected using the conventional biochemical analyzer. As shown in Table I, the serum levels of Cr and BUN significantly decreased in the miR-

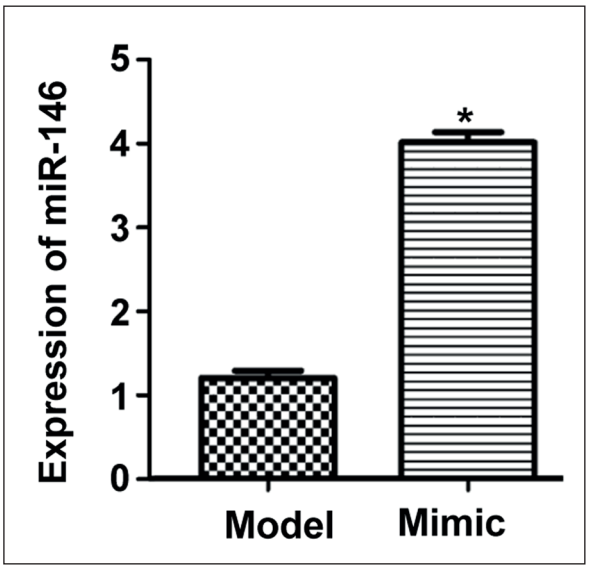

Figure 1. Expression of miR-146 in each group. Mimic: miR-146 Mimic group, *p<0.05 *vs.* control group and model group.

146 Mimic group, while they were elevated [illegible] model group (p<0.05). It is suggested th[illegible] functions in DN rats were improved by mi[illegible]6.

Effect of MiR-146 on NF-κB Signaling Pathway

The protein was extracted [illegible] tissues and detected *via* Western [illegible]ing. It [illegible]s found that the levels of p-IκB [illegible]-P65/P[illegible] markably upregulated [illegible] pared with those in [illegible] cont[illegible]up (p<0.01), while they signifi[illegible]y declined [illegible] miR-146 Mimic group c[illegible] with those [illegible] model group (p<0.0[illegible] The[illegible]lts of qPCR showed that the m[illegible]NA level of [illegible]had no significant differen[illegible]nong the three g[illegible] (N.S.), and the result[illegible]n imm[illegible]nohistochemical assay for the pos[illegible] expre[illegible] of p-IκB in tissues were consiste[illegible]th [illegible]protein [illegible]el as Western blotting revealed (Figure 2). The above findings demonstrated that the NF-κB signaling pathway could be activated in the model group by increasing the phosphorylation levels of IκB and P65. [illegible] DN-induced activation of the NF-[illegible]ignali[illegible] pathway could be inhibited in the [illegible]146 Mimic group.

Effects of MiR-146 on [illegible]ression [illegible]ls of Inflammatory Fac[illegible] TNF-α/IL-1β

The expression le[illegible] of TN[illegible]/IL-1β/I[illegible] in kidney tissues w[illegible] furth[illegible]etected using the ELISA kits. T[illegible]ni[illegible]up had [illegible]ently increased the l[illegible]s of T[illegible] IL-1[illegible]nd IL-6 compared wi[illegible]e control gr[illegible].01), while miR-146 [illegible]roup had e[illegible]ntly decreased their [illegible]els co[illegible]d with the model group (p<0.01) (Figure 3). T[illegible]ove results suggested tha[illegible]pression level[illegible]downstream cytokin[illegible] NF-α/IL-1β/IL-6 were markedly elevated [illegible]e model gr[illegible]after activation of the NF-κB [illegible]aling pathw[illegible] The overexpression of miR-1[illegible]ppressed [illegible]NF-κB signaling pathway and exp[illegible]f these cytokines.

Effect of MiR-146 on Apoptosis of [illegible] Tissues

[illegible] Annexin V-FITC and PI dual-fluorescence labeling for kidney tissues, apoptosis was detected using flow cytometry. It was found that the apoptosis was enhanced in the model group compared with that in the control group, while it was remarkably inhibited in the miR-146 Mimic group (Figure 4).

Discussion

MiRNAs are endogenous, non-coding, single-stranded, small RNA molecules generally with 19-22 nt in length[17,18], which can regulate the target gene expressions at the transcriptional level[7]. The maturation of miRNAs involves

Tab[illegible] Change[illegible]tent of Cr and BUN.

	Cr (μmol/L)	BUN (mmol/L)
[illegible]ontrol group	21.01 ± 3.11	7.23 ± 1.21
[illegible]del group	91.25 ± 2.34#	31.32 ± 3.14#
[illegible]46 Mimic group	36.66 ± 5.32*	14.24 ± 1.33*

Note: The content of Cr and BUN is decreased significantly in miR-146 Mimic group, while it is the opposite in model group (p<0.05). *p<0.05 *vs.* model group, #p<0.05 *vs.* control group.

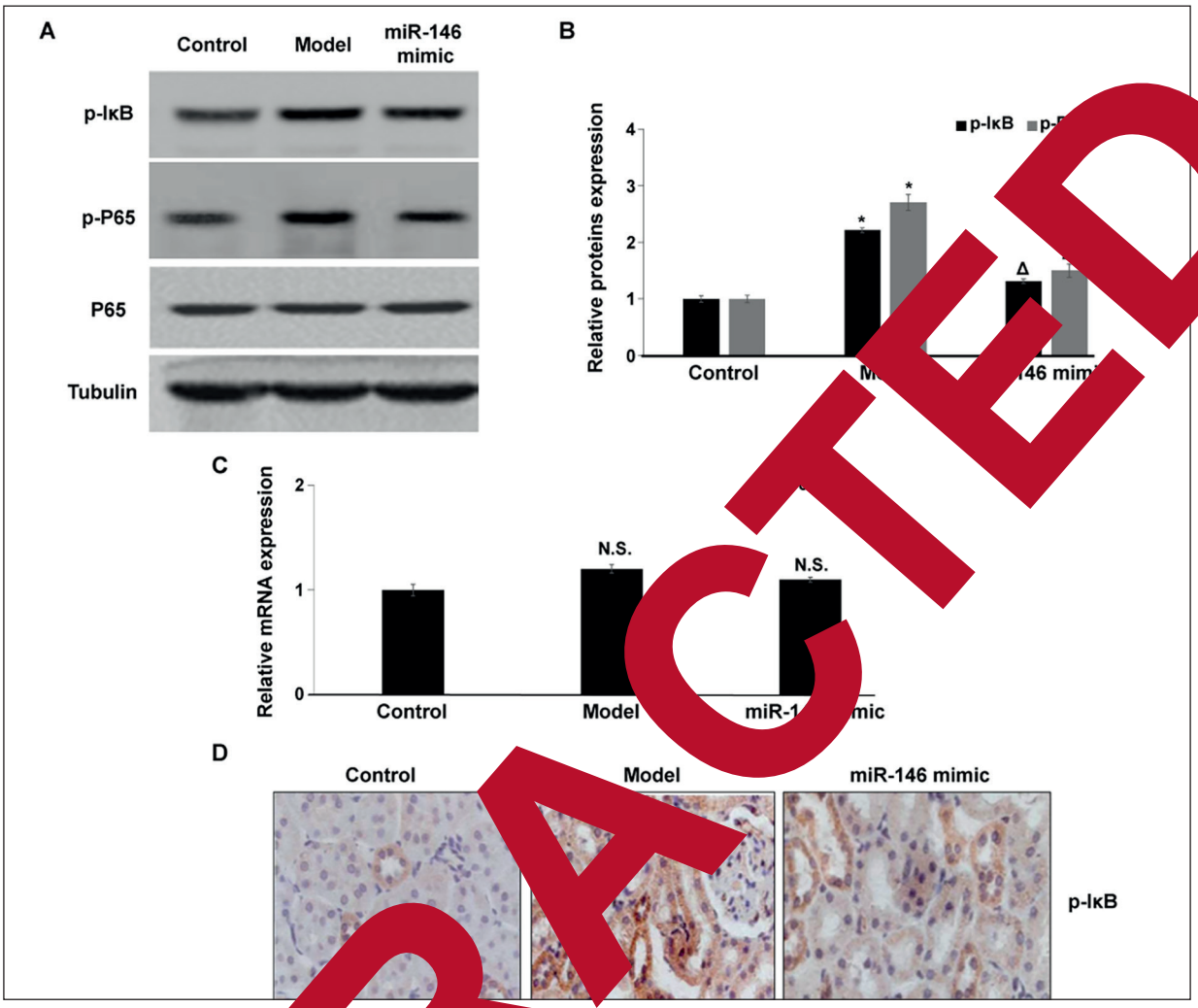

Figure 2. Effect of miR-1[illegible] on [illegible]. **A,** Protein levels of p-IκB, p-P65, P65 and Tubulin detected *via* Western blotting. **B,** Qu[illegible]cation [illegible], The mRNA level of P65 detected *via* qPCR. **D,** Positive expression of P-IκB in kidney tissues dete[illegible]*ia* immuno[illegible]emistry (magnification ´ 40). *p<0.01: model group *vs.* control group, $^{\Delta}p$<0.05: miR-146 Mimic gro[illegible]odel group.

two pro[illegible]s. First, Drosha [illegible]in and DGCR8 protei[illegible]ntly [illegible]ocess the [illegible]ranuclear pri-RNA [illegible]ecule[illegible]rming pre-miRNAs with 70 nt i[illegible]th[illegible]der th[illegible]tion of nuclear export protein [illegible]tin5/R[illegible]GTP, pre-miRNAs are [illegible]quen[illegible]an[illegible]ted from the nucleus to the [illegible]oplasm[illegible]y are further processed into mat[illegible] miRNA [illegible]olecules with about 21 nt in le[illegible]e assistance of Dicer. As a result, [illegible]NA molecules form the RNA-induced silencing complex through the target gene mRNA, [illegible]nhibiting or degrading the expression of the target genes[19].

MiR-146 is a widely studied miRNA currently, and it has been found to play an important role in regulating the cellular innate immunity. The binding sequences between promoter regions of NF-κB and miR-146 exist. LPS/TNF-α could stimulate the upregulation of miR-146, and subsequently, the expression levels of two target genes IRAK1 and TRAF6 are downregulated[20], thereby inhibiting the immunoinflammatory process. Therefore, it is believed that miR-146 regulates the inflammatory signaling pathway through negative feedback. In addition, miR-146 is involved in pathophysiological processes, such as autoimmune diseases, rheumatoid arthritis, inflammation, and breast cancer[21,22].

NF-κB, an important nuclear transcription factor, occupies a pivotal position in the inflam-

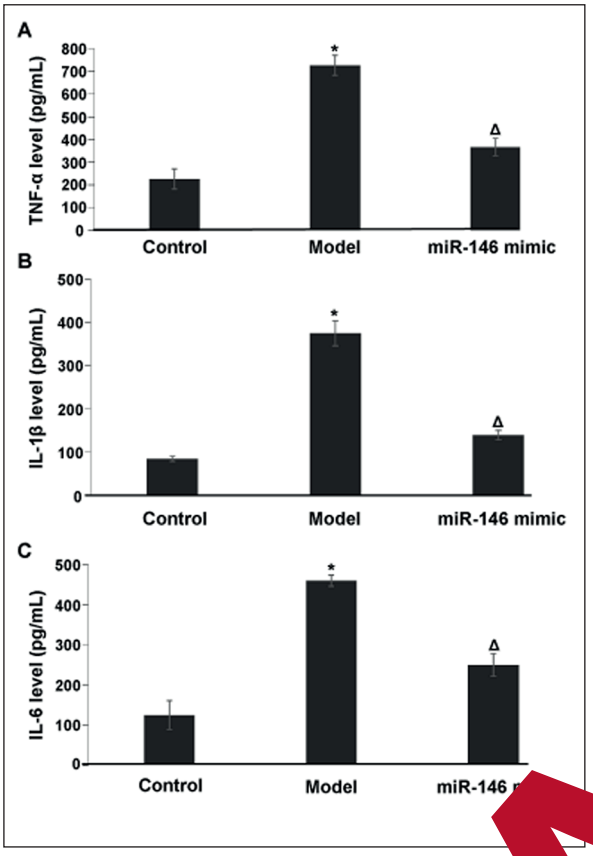

Figure 3. Effects of miR-146 on expression leve[l] inflammatory factors TNF-α/IL-1β/IL-6. **A,** TNF-α l[evel] detected. **B,** IL-1β level detected. **C,** [IL-6] level detecte[d]. *p<0.01: model group *vs.* control g[roup]; [#]p<0.05: miR-14[6] Mimic group *vs.* model group.

matory signaling p[athway]. W[hen] NF-κB enters the nucleus, the [tran]scription [of] variety of cellular inflam[matory] factors can [be] promoted, thereby medi[ating] the [in]cellular inflammatory response through inflammatory factors[23,24]. Under the resting state, NF-κB binds to IκB, and its subunits P65 and P50 form the dimer in the cytoplasm. After exogenous stimuli, su[ch as] TNF-α, and ROS, IκB is phosphoryl[ated] through signal transduction, and further d[egra]ded by the ubiquitinated proteasome, thereby [dis]integrating the NF-κB-IκB complex. The nucle[ar] NF-κB is activated, and the exposed [DNA-bind]ing protein [can] to specific sequences of tar[get] genes in the n[ucleus] thereafter, leading to [the] inflammat[ory] response by initiating the activit[y of] the [pro-]inflammatory factors[25-26]. As a res[ult], ac[ute] kidney inju[ry] can be caused due to t[he] NF-κB-a[ctiva]ted in[flam]matory response.

In the p[resent] study, SD rats w[ere] divided into control g[rou]p, mo[del] group, and miR-146 Mimic group. First, the ser[um] levels of kidney injury ind[ex] and BUN in [rats] were detected. The s[erum] levels of Cr and BUN significantly increased in the mod[el] group, while they remarkably [dec]reased in the m[iR]-146 Mimic group compared w[ith] those in th[e] model group, suggesting that the [kidney] injuries in DN rats could be alleviated by [miR-146]. Then, the effect of miR-146 on NF-κB signaling pathway was analyzed in the [three] groups. The results showed that the levels of p-IκB and p-P65 upregulated and the NF-κB signaling pathway was activated in the model group, which were inhibited in the miR-146 Mimic group. However, the above treatments had no significant effect on the mRNA level of P65. In addition, p-IκB level showed a similar trend. Furthermore, the effects of miR-146 on the expression levels of the downstream cytokines of NF-κB signaling pathway were detected using ELISA. The results revealed that the model group had evidently increased levels of TNF-α,

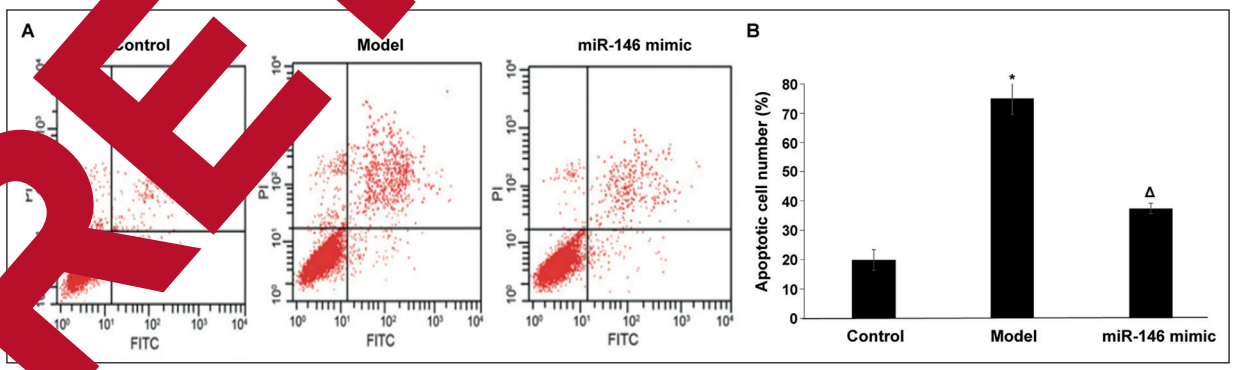

Figure 4. Effect of miR-146 on apoptosis of kidney tissues. **A,** Apoptosis determined using Annexin V-FITC and PI dual-fluorescence labeling and flow cytometry. **B,** Quantification of (**A**). *p<0.01: model group *vs.* control group, [#]p<0.05: miR-146 Mimic group *vs.* model group.

IL-1β and IL-6, while miR-146 Mimic group had evidently decreased levels compared with the model group. Finally, apoptosis was enhanced in the model group compared with that in the control group, while it was remarkably inhibited in the miR-146 Mimic group.

Conclusions

In summary, miR-146 can inhibit the NF-κB signaling pathway, lower the levels of TNF-α, IL-1β, and IL-6, and reduce the apoptosis, thereby exerting a protective effect against kidney injury in DN.

Conflict of Interest

The Authors declare that they have no conflict of interests.

References

1) Flyvbjerg A. The role of the complement sy… diabetic nephropathy. Nat Rev Nephrol 2… 311-318.
2) Tao Z, Shi A, Zhao J. Epidemiological perspec… of diabetes. Cell Biochem Biophys 2015; 73: … 185.
3) Kihm L. Hypertension and d… hropathy. Exp Clin Endocrinol Diabe… 2016; …1-2.
4) Sun H, Zhai Y. Assessm… of oxidat… tress injury with ischemia mo… albu… bined with fourier t… fo… spectros… py in patients wit… y diabe… hropathy. Acta Medica Med… 2019; 35: 3… 87.
5) Lim AK, Tes… flammation i… etic nephropathy… diato… mm 2012; 20…2: 146154.
6) Sun D… EN J, Yan X, … C, Tian H, Ji H, Lin S, Pe… , Jin L. Tripteryg… ilfordii polyglycosi… hibit the TGF-beta … -kappa b signal… athway… improve renal fibrosis in diabet… ephro… . Acta Medica Mediterr 2019; 35: …
7) Cai … Hu S, … A brief review on the mechanisms … RN… gulation. Genomics Proteom… Bioin… 2009; 7: 147-154.
8) …EHME KA, …LAUFFS B. Onset and progression … osteoarthritis-can growth factors, in… … cytokines, or differential miRNA expression concomitantly induce proliferation, ECM degradation, and inflammation in articular carti…ge? Int J Mol Sci 2018; 19. pii: 2282.
9) …UO J, Zeng X, Miao J, Liu C, Wei F, Liu D, Zheng Z, Ting K, Wang C, Liu Y. MiRNA-218 regulates osteoclast differentiation and inflammation response in periodontitis rats through Mmp9. Cell Microbiol 2019; 21: e12979.
10) Li F, Li D, Zhang M, Sun J, Li W, Jiang R, Han R, Wang Y, Tian Y, Kang X, Sun G. MiRNA… gets the GPAM gene and regulates… tiation of intramuscular adipocyte… ene 201… 685: 106-113.
11) Sun Y, An N, Li J, Xia J, Tian Y, Zh… X, Huang H, Gao J, Zhang X. MiRNA-206 reg… human pulmonary microvascula… othelia… op… tosis via targeting in c… c obstructive… nary disease. J Cell… hem 2…9; 120: … 6236.
12) Lederhuber H, Baer … …deghi K… rkner KR, Kasper DC… roH… tiny pla… n neonatal innate… unity? N… logy… ; 99: 51-56.
13) Nakasa… … Okubo A, H… ioto M, Nishida K, … M, … H. Expression of microRNA-146 in rheuma… rthritis synovial tissue. Ar… …eum 2008; … 34-1292.
14) … X, Cui S, Fu X, Liu … Wang Z, Liu Y. MicroRNA-146-5p promotes proliferation, migration and invasion in … cancer cells by targeting claudin-12. Cance… omark 2019; 25: 89-99.
15) …aumik D, S… GK, Schokrpur S, Patil CK, Camp… …Expression of microRNA-146 sup… …kappaB activity with reduction of metastatic potential in breast cancer cells. Oncogene 2008; 27: 5643-5647.
… Q, Li D, Han Y, Ding X, Xu T, Tang B. Mi…RNA-146 protects A549 and H1975 cells from LPS-induced apoptosis and inflammation injury. J Biosci 2017; 42: 637-645.
17) Bartel DP. MicroRNAs: genomics, biogenesis, mechanism, and function. Cell 2004; 116: 281-297.
18) Yan C, Wang J, Ni P, Lan W, Wu FX, Pan Y. DNRLMF-MDA: predicting microRNA-disease associations based on similarities of microRNAs and diseases. IEEE/ACM Trans Comput Biol Bioinform 2019; 16: 233-243.
19) Han J, Lee Y, Yeom KH, Kim YK, Jin H, Kim VN. The Drosha-DGCR8 complex in primary microRNA processing. Genes Dev 2004; 18: 3016-3027.
20) Zhang QB, Qing YF, Yin CC, Zhou L, Liu XS, Mi QS, Zhou JG. Mice with miR-146a deficiency develop severe gouty arthritis via dysregulation of TRAF 6, IRAK 1 and NALP3 inflammasome. Arthritis Res Ther 2018; 20: 45.
21) Petrovic N, Davidovic R, Bajic V, Obradovic M, Isenovic RE. MicroRNA in breast cancer: the association with BRCA1/2. Cancer Biomark 2017; 19: 119-128.
22) Li Y, Xu Y, Yu C, Zuo W. Associations of miR-146a and miR-146b expression and breast cancer in very young women. Cancer Biomark 2015; 15: 881-887.
23) Youssef M, Ibrahim A, Akashi K, Hossain MS. PUFA-Plasmalogens attenuate the LPS-induced ni-

tric oxide production by inhibiting the NF-kB, p38 MAPK and JNK pathways in microglial cells. Neuroscience 2019; 397: 18-30.

24) Aziz RS, Siddiqua A, Shahzad M, Shabbir A, Naseem N. Oxyresveratrol ameliorates ethanol-induced gastric ulcer via downregulation of IL-6, TNF-alpha, NF-kB, and COX-2 levels, and upregulation of TFF-2 levels. Biomed Pharmacother 2019; 110: 554-560.

25) Torres L, Serna E, Bosch A, Zaragozá R, García C, Miralles VJ, Sandoval J, Viña JR, García-Trevijano ER. NF-kB as node for signal amplification during weaning. Cell Physiol Biochem 2011; 28:

26) Ivanenkov YA, Balakin KV, Lavrovsky Y ecule inhibitors of NF-kB and JA AT signa transduction pathways as prom anti-inflammatory therapeutics. Mini Rev hem 2011; 11: 55-78.